Sensors and Materials, Vol. 34, No. 8 (2022) 3255–3269
MYU Tokyo

S & M 3039

Unmanned Aerial Vehicle 3D Trajectory Planning Based on Background of Complex Industrial Product Warehouse Inventory

Yuhang Han,[1] Qiyong Chen,[2] Nan Pan,[1*] Xiaojue Guo,[3] and Yuqiang An[4]

[1]Faculty of Civil Aviation and Aeronautics, Kunming University of Science and Technology, Kunming 650500, China
[2]Faculty of Material Science and Engineering, Kunming University of Science and Technology, Kunming 650500, China
[3]Kunming Zhiyuan Measurement and Control Technology Co., Ltd., Kunming 650500, P.R. China
[4]Logistics Center, Hongyun Honghe Tobacco (Group) Co., Ltd., Kunming 650202, P.R. China

(Received February 25, 2022; accepted July 15, 2022)

Keywords: industrial product warehouse, radio frequency identification, UAV, trajectory planning, fitness-adaptive differential evolution algorithm

Unmanned aerial vehicle (UAV) path planning is the key to the UAV carrying a high-precision portable radio frequency identification (RFID) reader to complete an inventory task. By taking a quadrotor UAV as the object, a type of method is proposed for the path planning using a UAV with RFID readers to conduct an inventory of industrial product warehouses. As the particle swarm optimization algorithm (PSO) tends to converge prematurely when solving path planning problems and tends to fall into local optima, PSO has been improved and an improvement method based on differential evolution has been proposed. The fitness-adaptive differential evolution algorithm (FiADE) and PSO are mixed and improved for further application in three-dimensional space. The final simulation results show that the hybrid suitability DE algorithm (PSO-DE) based on improved PSO has a higher uniformity than the DE algorithm, PSO, and whale optimization algorithm (WOA), and is more suitable for the trajectory planning of drones in complex industrial warehouses.

1. Introduction

Autonomous flight technology for unmanned aerial vehicle (UAV) has attracted considerable attention in the civilian sector. At present, four-rotor UAVs have been widely used in indoor positioning, photovoltaic inspection, pesticide spraying, inventory tasks, and environmental monitoring.[1,2] This study is based on the raw and auxiliary material warehouse environment of an industrial enterprise for planning the path of a four-rotor UAV inventory. For the UAV inventory task, the main difficulty lies in the following: the product information in the raw and auxiliary material warehouse is diverse, the quadrotor UAV used for warehouse inventory is limited in quantity, and the endurance is generally not strong. At the same time, it is also necessary to consider

*Corresponding author: e-mail: nanpan@kust.edu.cn
https://doi.org/10.18494/SAM3877

ISSN 0914-4935

issues such as obstacle avoidance. Therefore, reasonable UAV trajectory planning in the industrial warehouse environment can effectively improve the endurance and work efficiency of the quadrotor UAV.

At present, there are many research studies on UAV trajectory planning. At this stage, the algorithms to solve the UAV trajectory planning problem are mainly intelligent and accurate algorithms.[3,4] Taking the trajectory planning of UAVs as an example, Zhou *et al.*[5] used Bezier curves to generate the trajectory of a quadrotor UAV, but they did not study the motion model. The establishment of the dynamic model has no practical application value, as mentioned by Cheng *et al.*[6] Moreover, in related studies by Qian and Lei,[7] Gao *et al,*[8] Wang and Wang,[9] and Hu and Wu,[10] the traditional squid algorithm, fast-expanding random tree algorithm, traditional particle swarm optimization algorithm (PSO), and ant colony algorithm are not good enough for the convergence of the UAV trajectory planning problem, and the convergence speed is very low. The algorithm has been improved to enhance the optimization of the four above-mentioned algorithms and the ability to jump out of the local optimum, which has achieved certain results and has certain reference significance. However, these studies have mainly carried out simulation experiments for fixed-wing UAVs. Thus, the algorithm is not suitable for the trajectory planning of quadrotor UAVs. In addition, most of the research studies on UAVs at this stage only use the shortest flight path[11] or the least energy consumption[12] to establish a single-objective optimization model, and further use the convex approximation strategy[13] to calculate the track. The algorithm does not consider other target requirements during the drone mission process, which has certain limitations. In the obstacle avoidance link of UAV trajectory planning, the rapidly-exploring random trees (RRT) algorithm,[14] potential field method,[15] and other methods are often used.

At present, in most studies (e.g., Kumar *et al.*[16]), the path planning problem for UAVs is based on a two-dimensional environment, which causes difficulties in the practical application of the algorithm, and most of them do not have a track specifically for UAV inventory tasks. Their planning studies are based only on patrol missions, surveillance mission context,[17,18] and UAV trajectory planning. On the basis of the logistics distribution, Pei *et al.*[19] proposed a hybrid genetic algorithm based on the fusion extended K-means++ algorithm, and a dual-objective optimization model was established to reduce the time and energy spent in the UAV delivery process. On the basis of the background of UAV plant protection, Kan *et al.*[20] proposed an improved PSO to plan the operation path of a UAV and improve the operation efficiency of UAV plant protection operation. PSO is used to plan the UAV path.[21] In the literature,[22,23] the inventory task of quadrotor drones equipped with radio frequency identification (RFID) readers is explored, which has certain reference significance for the execution of the inventory tasks of drones, but there are problems such as incomplete and nonspecific mathematical models and task environment models.

Although relevant experts and scholars at home and abroad have conducted considerable research on UAV path planning, the following problems still exist:

1) To simplify the model, most of the research on UAV trajectory planning only focused on UAV trajectory planning under the two-dimensional model of the mission environment and did not involve the UAV trajectory planning research in the three-dimensional environment. The practical application of the algorithm caused difficulties.

2) Most of the current research studies have not applied UAVs to the actual industrial background and only remain at the theoretical level. The objective function is mostly a single objective function, which is too simple to consider other requirements of the task.
3) When studying the trajectory planning of a rotary-wing UAV, most studies did not add the physical constraints of the rotary-wing UAV and did not consider the unique aerodynamic characteristics of the rotary-wing UAV.

Therefore, the main research problem of this paper is UAV 3D trajectory planning based on a complex industrial product warehouse inventory background. To solve the above problems, this article is based on the background of quadrotor drones performing industrial product warehouse inventory tasks. Under the premise of meeting the power constraints of quadrotor drones, the structure of the inventory unit cargo has the least energy consumption and the highest accuracy rate. The objective function is to build a multi-objective optimization mathematical model to optimize the flight trajectory during the UAV inventory process. In this paper, we propose to use the improved fitness-adaptive differential evolution algorithm (FiADE) and PSO based on differential evolution. We introduce hybrid chaos strategies to improve the optimization performance of the PSO algorithm. The final simulation results show that the proposed algorithm outperforms PSO, the DE algorithm, and the whale optimization algorithm (WOA) and has a high degree of uniformity, enabling the inventory task to be completed effectively while avoiding obstacles.

2. Model Establishment

2.1 UAV motion model

Model assumptions:

1) Since the flying speed of the UAV is relatively low when performing the inventory flight task, the effects of the air resistances f_L, f_R, and f_D received by the UAV in level flight, ascending, and descending states, respectively, can be ignored.
2) Since the task environment of the quadrotor UAV is indoor during the mission, the airflow disturbance is not considered during the flight, and the effects of wind conditions are ignored.
3) When the aircraft is near the hovering state, we ignore the air drag moment in the hovering state to simplify the mathematical model of the quadrotor.
4) During the process of the UAV from the start (counting flight starting point) P_S to the end (counting flight ending point) P_E, the flight track T_{rack} can be decomposed into line segments between m nodes, $T_{rack} = \left\{T_{rackS}, T_{rack2}, ..., T_{rackj}, ..., T_{rackm-1}, T_{rackE}\right\}$.

$$F_\Omega - G = \begin{bmatrix} \ddot{x} \\ \ddot{y} \\ \ddot{z} \end{bmatrix}, \quad G = \begin{bmatrix} 0 \\ 0 \\ mg \end{bmatrix} \tag{1}$$

$$F_{\Omega i} = \sum \left(F_{Li} + F_{Ri} + F_{Di}\right) \tag{2}$$

$$a_i = \begin{bmatrix} 0 \\ 0 \\ -g \end{bmatrix} = \begin{bmatrix} \cos\theta & 0 & -\sin\theta \\ \sin\phi\sin\theta & \cos\phi & \sin\phi\cos\theta \\ \cos\phi\sin\theta & -\sin\phi & \cos\phi\cos\theta \end{bmatrix} \begin{bmatrix} a_x \\ a_y \\ a_z \end{bmatrix} \tag{3}$$

Among them, in Fig. 1, F_L, F_R, and F_D are the total lifts required by the UAV in level flight, ascending, and descending states, respectively. $F_{\Omega i}$ is the total rotor lift of the quadrotor UAV during the flight path segment i, a_i is the gravitational acceleration vector, and θ and Φ are the pitch and roll angles of the UAV, respectively.

$$\begin{cases} \theta = \arcsin\left(\dfrac{-a_x}{g}\right) \\ \phi = \arctan\left(\dfrac{a_y}{a_z}\right) \end{cases} \tag{4}$$

2.2 Constraints for quadrotor UAV

1) The maximum ascent speed and descent speed of the UAV during flight are determined by the physical performance of the UAV:

$$\begin{cases} v_{Rj} \le v_{R\max}, \\ v_{Dj} \le v_{D\max}. \end{cases} \tag{5}$$

2) The maximum pitch and roll angles that the UAV can fly during the pitch and roll movements are determined by the physical performance of the UAV:

$$\begin{cases} \theta_j \le \theta_{\max}, \\ \phi_j \le \phi_{\max}. \end{cases} \tag{6}$$

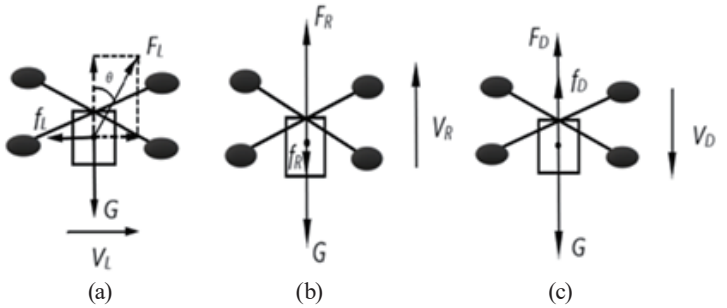

(a) (b) (c)

Fig. 1. Force analysis of UAV movement. (a) Level flight force. (b) Ascending force. (c) Drop force.

3) The longest time that the UAV can fly during an inventory task is determined by the physical performance of the UAV:

$$\sum t_j \le T_{\max}, \tag{7}$$

where t_j is the flight time of the jth trajectory.

2.3 Scanning model of RFID reader

The principle of the UAV carrying the RFID reader to collect product data is as follows. The RFID reader module on the UAV can achieve the purpose of inventory by scanning the electronic tags installed on the items and the cargo space. (Fig. 2)

When the drone carries the RFID reader into the product data collection, the raw and auxiliary materials to be counted are not only obstacles, but also need to meet the requirement that the tag is within the scanning range of the RFID reader carried by the drone to ensure that the original and auxiliary materials can be completed. In the material data collection task, when the UAV is at node j, $T_{racky} = (x_j, y_j, z_j)$, and we assume that the center coordinates C of the RFID tag of the ith cargo are (x_c, y_c, z_c). The UAV is expanded in a conical shape with the maximum scanning angle φ_{max} and the maximum scanning radius distance δ_{max}, and the establishment of UAV mission planning is based on RFID reading and writing the fitness function recognized by the machine:

$$l = \sqrt{\left(x_j - x_C\right)^2 + \left(y_j - y_C\right)^2 + \left(z_j - z_C\right)^2}, \tag{8}$$

$$\cos(\beta) = \frac{(0,0,1)\cdot\left(x_j - x_C, y_j - y_C, z_j - z_C\right)}{1\cdot\sqrt{\left(x_j - x_C\right)^2 + \left(y_j - y_C\right)^2 + \left(z_j - z_C\right)^2}}, \tag{9}$$

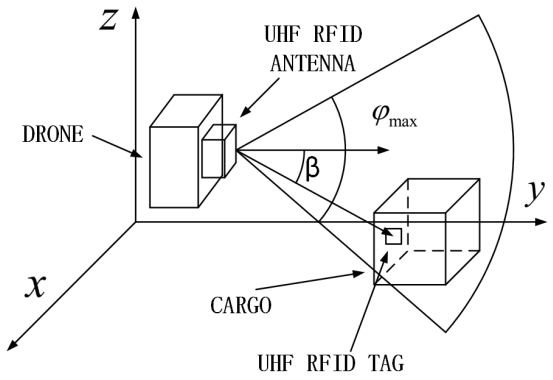

Fig. 2. Principle of UAV carrying RFID reader to collect product data.

$$U_i = \begin{cases} 1, & l \le \delta_{\max} \text{ and } 0 \le arc\cos(\beta) \le \varphi_{\max}, \\ 0, & \text{Others}, \end{cases} \tag{10}$$

$$U = \sum U_i . \tag{11}$$

2.4 UAV inventory of energy consumed per unit of cargo

The total energy consumed by the drone during the flight of the inventory mission is as follows:

$$P_{ower} = \sum_{j=1}^{n} \left(F_{Lj} + F_{Rj} + F_{Dj} \right) \cdot T_{rack\,j}, \tag{12}$$

$$K = \frac{\sum_{j=1}^{m} \left(F_{Lj} + F_{Rj} + F_{Dj} \right) \cdot T_{rack\,j}}{U}. \tag{13}$$

Therefore, the objective function in the article is

$$f = K \cdot \frac{1}{U}. \tag{14}$$

3. Algorithm Description

The path planning of the UAV can help the UAV complete the flight mission effectively and improve the operation efficiency. PSO is an evolutionary algorithm based on the foraging behavior of flying bird swarms, which can solve large-scale optimization problems. The algorithm treats birds as particles, and these particles form a particle swarm. Each particle has both speed and position attributes. A single particle adjusts its position according to its own optimal position and the optimal position of the entire group. After multiple iterations, the goal of optimization is achieved. PSO has simple calculations, high robustness, good memory, and high stability, which can be used to rapidly solve path planning problems. However, particle swarms are easy to converge prematurely and fall into local optimality, and the accuracy of path planning is often low. Therefore, in this paper, we propose to use the improved FiADE based on differential evolution to mix with PSO and introduce the chaos strategy to improve the optimization performance of PSO and effectively solve the complex environment in this paper.

In the use of the hybrid suitability DE algorithm (PSO-DE) to solve the three-dimensional path planning problem, we assume that each individual particle is

$$M_i^k (M_i^k = \{(x_1, y_1, z_1), (x_2, y_2, z_2), \cdots\} M_i^k = \{(x_1, y_1, z_1), (x_2, y_2, z_2), \cdots\} = \{m_1 + m_2 + \cdots\}),$$

where M_i^k represents the algorithm iteration to the position of the ith individual of the kth generation of the particle swarm, that is, the flight path of the UAV represented by the ith individual. In the iterative process, the particle swarm continuously updates and evolves and moves toward the optimal solution.

3.1 Basic step of algorithm

For the FiADE algorithm, the update strategy is as follows.

3.1.1 Mutation operation

For each target vector in the population $M_{i,E}$, E means that the algorithm runs to the Eth generation to perform differential mutation operation [Eq. (15)] and the generated mutation vector is denoted as $V_{i,E} = [V^1{}_{i.G}, ..., V^D{}_{i.G}]$.

$$V_{i,E} = M_{r_1^i,E} + F_i \cdot (M_{r_2^i,E} - M_{r_3^i,E}) + F_i \cdot (M_{r_4^i,E} - M_{r_5^i,E}) \tag{15}$$

In the formula, the subscripts $r^i{}_1$, $r^i{}_2$, $r^i{}_3$, $r^i{}_4$, and $r^i{}_5$ are randomly selected individual serial numbers between $[1, N_p]$ and different from i, and F_i is the scaling factor corresponding to individual i. The calculation process is as follows.

Step 1: Calculate F_i for each individual M_i.

$$F_1 = F_{\max} \cdot \left(\frac{\Delta f_i}{\lambda_{con} + \Delta f_i} \right) \tag{16}$$

In the formula, $\Delta f_i = |f(X_i) - v(X_{best})|$ and M_{best} are the lowest fitness individuals $\lambda_{con} = 0.1 \times \Delta f_i + 10^{-14}$ in the current population, and F_{max} is the given parameter.

Step 2: Calculate F_2 for each individual M_i.

$$F_2 = F_{\max} \cdot (1 - e^{-\Delta f_i}) \tag{17}$$

Step 3: Calculate F_i .

$$F_i = \max(F_1, F_2) \tag{18}$$

3.1.2 Cross operation

The target vector $M_{i,E}$ and its corresponding mutation vector $V_{i,E}$ execute the crossover strategy, the newly generated individual is denoted as $U_{i,E} = \{u_{i,E}^1, u_{i,E}^2 \cdots u_{i,E}^D\}$, and the calculation formula for the jth point $u^i{}_{i,E}$ in individual i is

$$u_{i,G}^{j} = \begin{cases} v_{i,E}^{j}, & \text{if } rand(0,1) \le CR_i, \\ m_{i,E}^{j}, & \text{otherwise.} \end{cases} \tag{19}$$

In the formula, CR_i is the crossover probability corresponding to individual i, and the calculation process is as follows. Compare the fitness function value of the mutation vector V_i and the original vector M_{best}; if $f(V_i) < f(M_{best})$, execute Eq. (20); otherwise, execute Eq. (21).

$$CR_i = CR_{const} \tag{20}$$

$$CR_i = CR_{\min} + \frac{CR_{\max} - CR_{\min}}{1 + \left| f(V_i) - f(M_{best}) \right|} \tag{21}$$

Here, CR_{const}, CR_{min}, and CR_{max} are the set parameters.

3.1.3 Select operation

Comparing the original individual $M_{i,E}$ with the fitness function value of the new individual $U_{i,E}$ after mutation and crossover operation, we select individuals using Eq. (22). The superior individual enters the next cycle and the weaker individual is eliminated.

$$M_{i,E} = \begin{cases} U_{i,E}, & \text{if } f(U_{i,E}) \le f(M_{i,E}) \\ M_{i,E}, & \text{otherwise} \end{cases} \tag{22}$$

For individual particle swarm positions, the update strategy is as follows.

The new individuals optimized by FiADE are used as contemporary individuals of the particle swarm to participate in the position update of the particle swarm to produce offspring individuals.

$$v_i^{k+1} = \omega \times v_i^k + c_1 \times Rn \times (p_i - M_i^k) + c_2 \times Rn \times (g - M_i^k) \tag{23}$$

$$M_i^{k+1} = M_i^{k+1} + v_i^{k+1} \tag{24}$$

Among them, $v^k{}_i$ represents the flight speed of the ith individual in the kth iteration, ω is the inertia factor, c_1 and c_2 are the learning factors, p_i is the historical optimal position of the ith particle swarm individual, and g is the global optimal position.

To prevent the particle swarm from falling into the local extreme point, the chaos optimization idea is introduced into PSO. We perform chaotic optimization on the global optimal position $g = (g_1, g_2, \ldots)$ and map g_1 to the domain [0, 1] of the logistic equation to obtain Z_i. The logistic equation is

$$Z_{n+1} = \mu Z_n (1 - Z_n) \quad (n = 0,1,2,\cdots). \tag{25}$$

Then, we use the logistic equation to iteratively generate the chaotic variable sequence

$$Z_i^{(m)} (m = 0,1,2,\cdots). \tag{26}$$

Then, the generated chaotic variable sequence $Z_i^{(m)}$ is restored to the original solution space through inverse mapping to obtain $G^{(m)}$, the fitness function value of the sequence is calculated, and the individual position of the optimal fitness value is substituted for *g*.

To ensure that the number of populations remains unchanged after merging, some individuals are eliminated by roulette operation after the fitness value is normalized. Compared with traditional algorithms, FiADE can dynamically adjust the scaling factor and crossover probability of the DE algorithm according to the change in the individual fitness function value of each generation of population and balance the development and exploration capabilities of the algorithm. The new individuals generated by FiADE are added to the particle swarm, which improves the diversity of the population and makes the algorithm have the advantages of PSO and the DE algorithm.

3.2 Basic steps of the algorithm for solving the irregular placement model

(1) Initialization parameters

Initialize the parameters included in the algorithm.

(2) Initialize the track point

The RRT algorithm is used to generate the initial collision-free trajectory and obtain an initial feasible path. A polynomial fitting method is used to perform segmental fitting on the initial path, and the segment lengths are the same.

(3) Variation

Use the mutation operation in FiADE to randomly select five individuals in the population and perform the mutation operation.

(4) Cross

Perform a crossover strategy between the mutation vector generated in 3.2 (3) and the corresponding individual position to generate a new individual.

(5) Foraging

After the offspring are produced, they participate in the particle swarm update strategy, and the offspring follow their parents for food.

(6) Update the global and individual extreme values.

Update the global and individual optimal values, and record the global optimal path *g* and the individual optimal path p_i. Judge whether the maximum number of iterations is reached; if it is reached, exit the loop and output the optimal path; if not, return to 3.2 (3). (Fig. 3)

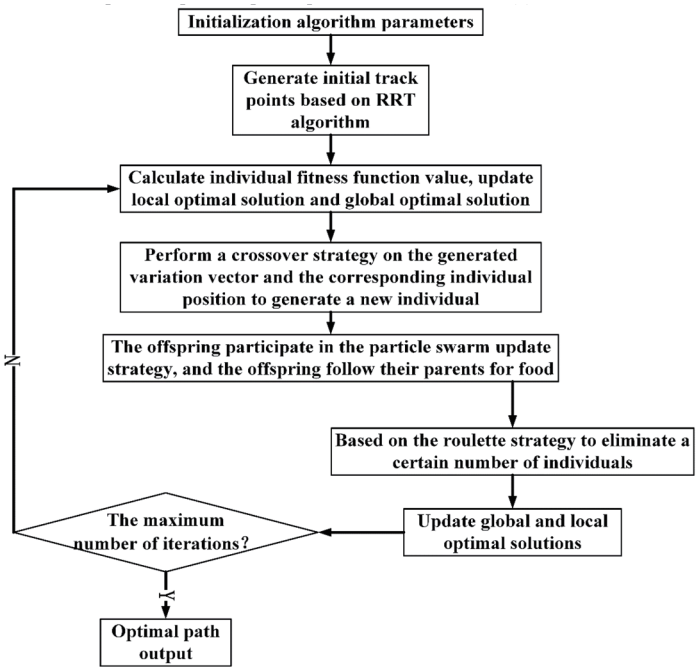

Fig. 3. Algorithm basic flow chart.

3.3 Simulation verification and analysis

We conducted simulation verification for the above-mentioned improved PSO. The simulation software is MATLAB2017a, and the relevant three-dimensional model is established on the basis of the physical map of the industrial warehouse, as shown in Fig. 4. By extracting the parameters of a drone and an RFID reader, the relevant parameters of the drone and RFID can be obtained: v_{Rmax} = 2.5 m/s , v_{Dmax} = 1.5 m/s, T_{max} = 1800 s, δ_{max} = 5 m, and Φ_{max} = 120°. In simulation verification, the parameter settings are shown in Table 1. The coordinates of the flight start point of the UAV are (0, 0, 0), and the coordinates of the flight end point are (0, 60, 0). First, we verify the ability of the proposed algorithm to avoid obstacles, as shown in Fig. 5. Secondly, under the condition of ensuring the safe flight of the quadrotor UAV, we verify the storage efficiency and accuracy of the quadrotor UAV, as shown in Tables 2 and 3, and Fig. 6.

3.4 Simulation environment for quadrotor UAVs to perform disk library tasks

The environmental model of the UAV performing raw and auxiliary material inventory tasks in a warehouse is shown in Fig. 4. To verify the advantages of the algorithm proposed in this paper, three other algorithms such as PSO are selected as experimental comparison examples. We compare them with the PSO-DE proposed in this paper for verification.

3.5 Simulation results of quadrotor UAV performing disk library task

In the process of running PSO-DE, PSO, DE, and WOA 30 times, the simulation results are shown in Tables 2 and 3.

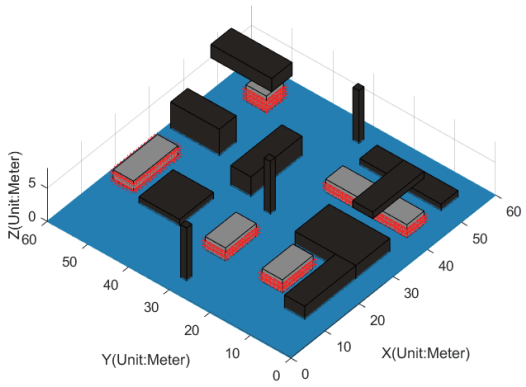

Fig. 4. (Color online) Schematic diagram of raw and auxiliary material warehouse scene.

Table 1
Parameter setting table.

Parameter	G_{max}	N_{max}	F_{max}	CR_{const}	CR_{min}	CR_{max}	NP	ω
Value	150	20	0.75	0.85	0.1	0.8	20	0.6

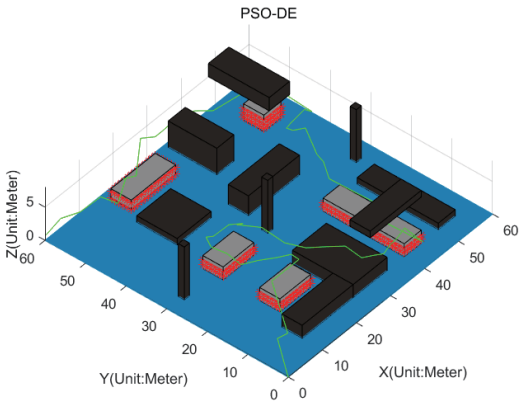

Fig. 5. (Color online) PSO-DE algorithm inventory roadmap.

Table 2
Cargo information collection results of four algorithms (PSO-DE, PSO, DE, and WOA).

Index	Algorithm			
	DE	PSO	WOA	PSO-DE
Quantity of collected goods	691	694	695	708
Cargo collection rate (%)	89.97	90.36	90.49	92.19
Inventory speed (s/box)	0.1259	0.1346	0.1346	0.1225

Table 3
Average cargo information collection results of four algorithms running thirty times.

Index	Algorithm			
	DE	PSO	WOA	PSO-DE
Average fitness value	1.067	1.126	1.147	1.024
Average cargo collection	688	691	694	702
Average cargo collection rate (%)	89.58	89.97	90.36	91.41

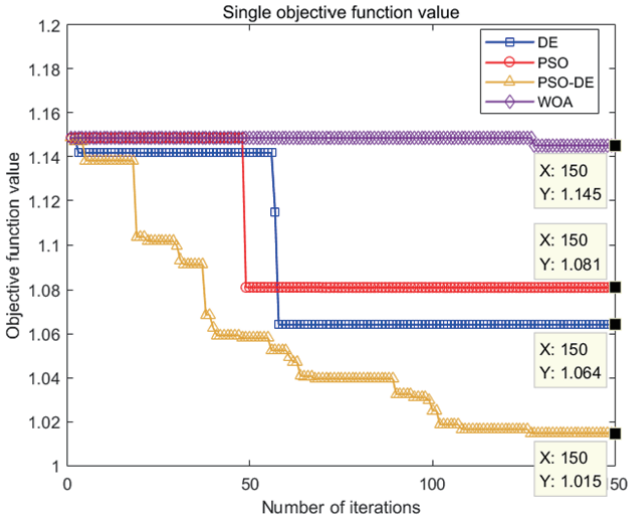

Fig. 6. (Color online) Curve of objective function value with the number of iterations.

3.6 Simulation analysis of quadrotor UAV performing warehouse inventory task

It can be seen from the simulation results shown in Fig. 5 that the trajectory planned by PSO-DE designed in this paper can effectively adapt to the three-dimensional warehouse environment, avoid obstacles in the warehouse environment, and complete the warehouse inventory task. For different obstacle models, the UAV can effectively avoid obstacles to reach the target point, thus verifying the effectiveness of the algorithm, and the planned path is suitable for UAV flight. It can be seen from Fig. 6 that the proposed algorithm has the highest convergence speed, the best convergence effect, and a certain degree of uniformity. Therefore, the algorithm not only retains the robustness, memory, and stability of PSO, but also overcomes the problems of premature convergence and easiness in falling into local optimum, and improves the accuracy of path planning.

Tables 2 and 3 show that in the process of running the algorithm 30 times, the statistical results indicate that, in the average of the 30 runs, when the maximum fitness function value differs from the minimum fitness function value by about 10%, the difference between the maximum cargo scanning rate and the minimum cargo scanning rate is 1.83%. The cargo scanning rates are similar, but the difference in response function value is large. Moreover, according to the improved method proposed in this article, the flight data of the UAV are detected in the field, and the average flight time is increased by 20%. Therefore, according to the multi-objective function in the article, it can be concluded that the FiADE–PSO hybrid algorithm with the introduction of the chaos strategy proposed in this article can effectively reduce energy consumption while ensuring the accuracy of cargo scanning, which can effectively use the battery life of the quadrotor UAV.

4. Conclusions

For the 3D trajectory planning problem of the inventory flight of a UAV with an RFID reader, we proposed a hybrid improved FiADE algorithm and PSO to further extend it to 3D space with a quadrotor UAV as the object. Our works are as follows.

1) We analyzed the movement and dynamics of the UAV, simplified its three-dimensional movement process, established the corresponding mathematical model, and obtained the physical performance constraints of the quadrotor UAV, which provided conditions for the in-depth study of the UAV trajectory planning problem.
2) We established a multi-objective function with the highest inventory rate of raw and auxiliary materials and the lowest energy consumption per unit of inventory, which effectively solved the inventory task of drones with RFID readers.
3) We mixed the improved FiADE and PSO based on differential evolution, then introduced the chaos strategy to improve the performance of PSO and reduce the energy consumption of the UAV inventory task. We improved the effective endurance time and effectively solved the problem of the UAV library in a complex environment.

In the next stage, we will further study the trajectory planning of multiple UAVs with dynamic obstacles in the inventory process and study autonomous flight strategies. On the basis of our findings, we will add further interference threats such as sudden obstacle threats and RFID interference source threats, which will be suitable for complex and suddenly changing warehouse environments.

Acknowledgments

This work was supported in part by the technology project of Hongyun Honghe Tobacco (Group) Co., Ltd. under Grant nos. HYHH2020XX03 and HYHH2021XX04.

References

1 S. Duangsuwan and P. Jamjareekulgarn: Sens. Mater. 32 (2020) 511. https://doi.org/10.18494/SAM.2020.2450
2 W. You, F. Li, L. Liao, and M. Huang: IEEE Access 8 (2020) 64971. https://doi.org/10.1109/ACCESS.2020.2985053
3 W. Shan, N. Cui, B. Huang, X. Wang, and Y. Bai: J. Chinese Inertial Technology 28 (2020) 122. https://doi.org/10.13695/j.cnki.12-1222/o3.2020.01.019 (in Chinese).
4 G. Liu , W. Jiang, W. Tan, and X. Lan: Sens. Mater. 32 (2020) 1141. https://doi.org/10.18494/SAM.2020.2525
5 W. Zhou, X. Wang, H. Sun, and Y. Chen: J. Instrum. 33 (2019) 53. https://doi.org/10.13382/j.jemi.b1902198 (in Chinese).
6 H. Cheng, S. Yang, and X. Qi: Comput. Eng. Design 39 (2018) 3705. https://doi.org/10.16208/j.issn1000-7024.2018.12.019 (in Chinese).
7 Z. Qian and M. Lei: J. Harbin Inst. Technol. 51 (2019) 37. https://doi.org/10.11918/j.issn.0367-6234.201805004 (in Chinese).
8 S. Gao, J. Ai, and Z. Wang: J. Syst. Eng. Electron. 42 (2020). https://doi.org/101.10.3969/j.issn.1001-506X.2020.01.14 (in Chinese).
9 Y. Wang and S. Wang: Comput. Eng. Sci. 42 (2020) 1690. https://doi.org/10.3969/j.issn.1007-130X.2020.09.020 (in Chinese).
10 S. T. Hu and Y. Wu: Hangkong Xuebao (2020) 1. https://doi.org/10.7527/S1000-6893.2020.24383 (in Chinese).
11 M. Samir, S. Sharafeddine, C. M. Assi, T. M. Nguyen, and A. Ghrayeb: IEEE Trans. Wirel. Commun. 19 (2019) 34. https://doi.org/10.1109/TWC.2019.2940447
12 J. Seongah, S. Osvaldo, and K. Joonhyuk: IEEE Trans. Veh. Technol. 67 (2017) 2049. https://doi.org/10.1109/TVT.2017.2706308
13 H. Wang, J. Wang, G. Ding, J. Chen, F. Gao, and Z. Han: IEEE Trans. Wirel. 18 (2019) 3485. https://doi.org/10.1109/TWC.2019.2914203
14 X. Zhou, X. Yu, and X. Peng: IEEE Trans. Aerosp. Electron. Syst. 55 (2019) 1743. https://doi.org/10.1109/TAES.2018.2875556
15 C. Yuan, S. Weng, Y. He, J. Shen, L. Chen, and T. Wang: Nongye Jixie Xuebao 50 (2019) 394 (in Chinese). https://doi.org/10.6041/j.issn.1000-1298.2019.09.046

16 P. Kumar, S. Garg, A. Singh, S. Batra, N. Kumar, and I. You: IEEE Internet Things J. 5 (2018) 1698. https://doi.org/10.1109/JIOT.2018.2796243
17 R. Wai and A. S. Prasetia: IEEE Access 7 (2019) 126137. https://doi.org/10.1109/ACCESS.2019.2938273
18 J. Li, Y. Xiong, J. She, and M. Wu: IEEE Internet Things J. 7 (2020) 8967. https://doi.org/10.1109/JIOT.2020.2999083
19 S. Pei, T. Shen, Z. Ning, and Y. Xie: Syst. Eng. 39 (2019) 3111. https://doi.org/10.12011/1000-6788-2018-0679-09 (in Chinese).
20 P. Kan , Z. L. Jiang, Y. H. Liu, and Z. W. Wang: Hangkong Xuebao 41 (2020) 323610 (in Chinese). https://doi.org/10.7527/S1000-6893.2019.23610
21 Y. Wang, P. Bai, X. Liang, W. Wang, J. Zhang, and Q. Fu: IEEE Access 7 (2019) 105086. https://doi.org/10.1109/ACCESS.2019.2932008
22 J. X. Lu, L. B. Zhao, and H. T. Tang: Int. J. Comput. Integr. Manuf. 24 (2018) 3129. https://doi.org/10.13196/j.cims.2018.12.020
23 H. Liu, Q. Chen, N. Pan, Y. Sun, Y. An, and D. Pan: IEEE Trans. Ind. Inf. 18 (2022) 582. https://doi.org/10.1109/TII.2021.3054172

About the Authors

Yuhang Han is an undergraduate student in the Faculty of Civil Aviation and Aeronautics, Kunming University of Science & Technology. His main research directions are swarm intelligence and deep learning.

Qiyong Chen is an undergraduate student in the Faculty of Materials Science and Engineering, Kunming University of Science & Technology. His main research directions are swarm intelligence and deep learning.

Nan Pan received his B.Sc. degree in 2008 from Anhui University of Science and Technology and his Ph.D. degree in 2012 from Kunming University of Science and Technology. From 2013 to 2017, he was a lecturer with the Faculty of Mechanical & Electrical Engineering, Kunming University of Science & Technology. From 2017 to the present, he is an associate professor with the Faculty of Civil Aviation and Aeronautics of Kunming University of Science & Technology. He is the author of more than 100 articles and holds more than 100 patents. His research interests include swarm intelligence and deep learning. He was selected as one of the Kunming young academic and technical leaders in 2018, top young talents in Yunnan in 2019, and high-end talents introduced in Yunnan Province in 2020.

Xiaojue Guo received her B.S. degree in 2013 from Nanjing University of Finance and Economics and her M.S. degree in 2017 from East China University of Political Science and Law. She is now the general manager of Kunming Zhiyuan Measurement and Control Technology Co., Ltd. Her main research directions are project management and intellectual property.

Yuqiang An received his M.S. degree from Kunming University of Science & Technology in July 2011. From 2011 to the present, he is a deputy chief and engineer of Hongyun Honghe Tobacco (Group) Co., Ltd. His main research directions are artificial intelligence and intelligent systems.